

An overview of the physico-chemical characteristics of dust at Kanpur in the central Indo-Gangetic basin



Amit Misra^{a,*}, Abhishek Gaur^a, Deepika Bhattu^a, Subhasish Ghosh^a, Anubhav Kumar Dwivedi^a, Rosalin Dalai^a, Debajyoti Paul^a, Tarun Gupta^a, Vinod Tare^a, Sumit Kumar Mishra^b, Sukhvir Singh^b, Sachchida Nand Tripathi^a

^a Department of Civil Engineering, Indian Institute of Technology Kanpur, India

^b National Physical Laboratory, New Delhi, India

HIGHLIGHTS

- Characterisation of dust properties in pre-monsoon season from in-situ measurement.
- A novel classification scheme proposed for aerosol types with focus on dust.
- Classification consistent with measured aerosol properties, and back-trajectories.

ARTICLE INFO

Article history:

Received 10 March 2014

Received in revised form

16 August 2014

Accepted 19 August 2014

Available online 20 August 2014

Keywords:

Dust

Indo-Gangetic basin

Aerosol classification

ABSTRACT

The optical, chemical, and physical properties of dust over the Indo-Gangetic basin are presented based on a campaign mode experiment conducted at Kanpur (26.52°N, 80.23°E), India, during April to July, 2011. During the study period, heavy dust storms and onset of south-west Indian Monsoon occurred. Based on physico-chemical characteristics, four aerosol types were identified in the region: background aerosol, dust dominated aerosol, pollution dominated aerosol, and mixed aerosol. The classification of aerosol types was found to be consistent with various aerosol properties examined and backtrajectory analysis. In addition to the locally generated aerosols, there were both short and long range transported aerosols. Aerosols of oceanic origin were encountered during late June, and July.

© 2014 Elsevier Ltd. All rights reserved.

1. Introduction

Dust is an important component of atmospheric aerosols and plays an important role in cloud condensation nuclei (CCN) (Karydis et al., 2011; Zhang et al., 2009), impact on health (Karanasiou et al., 2012; Onishi et al., 2012), radiative properties (Dey et al., 2004), and atmospheric composition (Chinnam et al., 2006). Satellite and ground-based remote sensing has been proven to be an invaluable tool in studying the long-term variation and transport of dust (Kaufman et al., 2005). However, detailed understanding of dust microphysical and chemical properties can be obtained only from advancement in in-situ measurements and analysis. Uncertainties in the properties of dust are related to particle size, shape, and chemical composition (Chen et al., 2011). There is a large variability in dust chemical composition and

relative abundance of elements with respect to source and transport. Studies have been performed to utilize this aspect to identify the dust sources and transport pathways. Formenti et al. (2011) reviewed the role, importance and uncertainty of dust in the atmosphere.

The Indo-Gangetic basin is a region prone to dust during the pre-monsoon season (Chinnam et al., 2006; Mishra and Tripathi, 2008). This is either due to transport, both from and to the neighbouring dust-dominated regions, as a result of the high winds prevalent during this season, or local release, either from dry agricultural fields when left barren after the harvest, or the roadside dust (Giles et al., 2011). The dust from both agricultural fields and roadside are lifted off when sufficiently high wind speeds are attained. However, as compared to other dust-dominated locations, the Indo-Gangetic basin does not contain 'clean' dust (by 'clean dust', we mean dust without any mixing with pollution). Because there are several industrial and mega-cities in this region, there is considerable amount of pollution originating from industrial and

* Corresponding author.

E-mail addresses: sri.amit.misra@gmail.com (A. Misra), snt@iitk.ac.in (S.N. Tripathi).



Fig. 1. Map of northern India showing the study location. The background image was obtained from Google Earth.

vehicular emissions. There could also be remnants of burning of agricultural fields after harvest in early pre-monsoon. During April and May, forest fires are also common in Nepal region, located to the north of the study area. Under conducive circumstances, the finer particles can be transported to the Indo-Gangetic region. Besides, as observed in this study, during the south-west monsoon season, sea salt aerosols also contribute to the overall aerosol burden, especially during late pre-monsoon season. Hence, the aerosol climatology in the Indo-Gangetic basin during pre-monsoon season encompasses a mixture of different aerosol types. The dominant species also change with the progress of season. Hence, the aerosol model for this region during pre-monsoon season is complicated, and assuming a simplified model for radiative transfer computation and other studies would result in uncertainty.

Several studies have been carried out to study dust properties and behaviour in general (Reid et al., 2003, 2008; Chen et al., 2011) and during storms (Thorsteinsson et al., 2011). Studies have also been carried out in the Indo-Gangetic basin (Chinnam et al., 2006; Dey et al., 2004) especially using ground based remote sensing instruments (Aerosol Robotic Network) (Dey et al., 2004; Giles et al., 2011). Eck et al. (2010) also studied the Kanpur data for the entire range of fine mode fractions, including dust dominated observations.

This paper reports results of a four-month (April to July 2011) experiment, conducted at the Indian Institute of Technology, Kanpur (IITK), India, for characterisation of dust prevalent over the Indo-Gangetic basin. Various types of in-situ instruments were used in this study for measurement of different aerosol properties. The underlying idea was to examine the mixing of dust with other aerosol types with the aid of simultaneous measurements of physical and chemical properties of aerosols. Modification in the

aerosol loading, and physical, optical and chemical properties of aerosols due to enhanced dust release and pollution was also studied. First, we describe the study area, and the general meteorology prevalent over the region during the pre-monsoon season. This is followed by a description of the methodology i.e. the instrumentation, and analytical protocols followed. In the results and discussion section, first the classification of aerosol types into different categories is presented, which is followed by an inter-comparison of different properties for these aerosol categories.

2. Site description and meteorology

The Indo-Gangetic basin is a large region in north India with an area of about 653,211 km², and accommodates about 41.3% of the total Indian population (Chowdhury et al., 2012). With large number of major Indian rivers, the basin is highly irrigated. Two metropolitan cities, Delhi and Kolkata, and several other rising centres of industrial activity and economic growth e.g. Chandigarh, Kanpur, Ranchi are located in the Indo-Gangetic basin (Fig. 1). The region witnesses large spatial heterogeneity with regard to aerosol type and land use (Choudhry et al., 2012).

Fig. 2 shows the wind rose diagram for the measurement site during April–July 2011 study period. The wind data was obtained from the National Centre for Environmental Prediction (NCEP) Reanalysis project (Kalnay et al., 1996). Winds were northerly and north-easterly in April; and north-westerly, northerly, and north-easterly in May. Thus, during April and May, aerosols sampled at the study location were mainly of continental origin as there is no sea or ocean to the north, north-west or north-east direction of the site. During June, the winds were north-easterly and easterly, whereas in July, they were mainly easterly. Thus, in addition to aerosols of continental origin, during June and July there is a

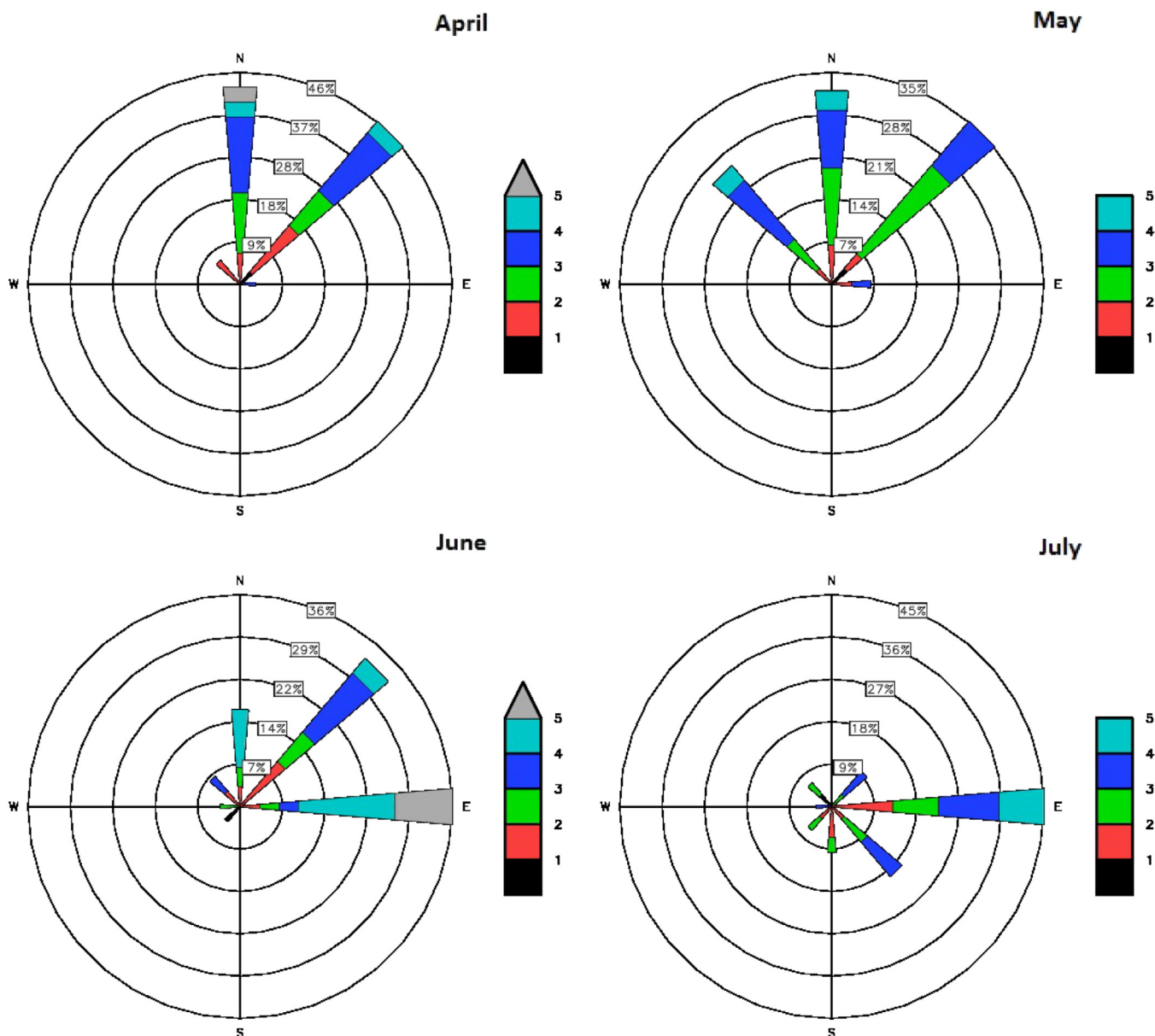


Fig. 2. Wind rose diagram for April, May, June, and July 2011 during the four-month campaign period.

possibility of aerosols transported from the Bay of Bengal and delta region of Ganga. Late June, and July witness onset and continuation of monsoon.

Besides the local emission of aerosols, there is horizontal as well as vertical transport that also bring in aerosols from neighbouring regions. Mostly due to the prevailing wind conditions, air mass is lifted to greater heights upto 4 km, during pre-monsoon months. During this season, occasional layer of dust is also seen, which subsides with the onset of monsoon. During winter months, most of the aerosols are concentrated near the surface below 1 km altitude (Misra et al., 2012; Tripathi et al., 2005).

Fig. 3 shows the ambient relative humidity (RH) and temperature measured using the Vaisala temperature and RH sensor (Vaisala, Inc. Humicap, HMT 337, accuracy of $\pm 1\%$) at Kanpur during April to July, 2011. The monthly-average temperature obtained for April, May, June, and July, 2011, was 35.4 ± 2.5 °C, 39.2 ± 2.2 °C, 32.8 ± 5.0 °C, and 32.6 ± 2.5 °C, respectively. The maximum temperature ($T_{\max} = 42.1$ °C) was in May and minimum ($T_{\min} = 26.1$ °C)

in June. Monsoon period showed higher temperature gradient compared to pre-monsoon (April, May). RH was generally high on rainy days and crossed 60% on cloudy days. It was observed that temperature was always greater than 30 °C in May, and subsequently temperature decreased and RH increased. Higher variation in RH and temperature was seen during June and July. Year 2011 was a normal monsoon year, with monthly rainfall over India being 112%, 85%, 109% and 108% of long period average (LPA) during June, July, August, and September, respectively (Monsoon Report, 2011, Indian Meteorological Department, Ministry of Earth Sciences, Government of India). The LPA (= 89 cm) of southwest monsoon is defined on the basis of 1951–2000 rainfall data.

Kaskaoutis et al. (2013) have used AERONET data to study the aerosol properties during severe aerosol loading conditions at Kanpur. They found that the coarse mode aerosols at Kanpur during pre-monsoon and monsoon season are three times the seasonal mean, implying that the enhanced aerosol optical depth (AOD) during these seasons is mainly contributed by coarse mode

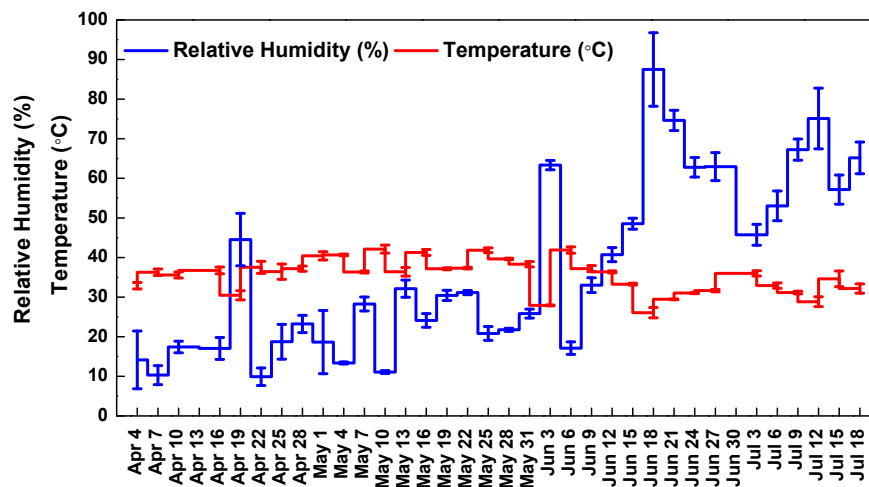


Fig. 3. Variation in temperature and relative humidity during the campaign period. Error bars represent 1σ deviation.

aerosols. Tiwari et al. (2013) have studied the heterogeneity in aerosol properties in pre-monsoon season along the Indo-Gangetic basin (IGB) using AERONET data from multiple stations. They found that the aerosols in the western IGB are dominated by coarse mode particles and those in the eastern IGB by fine mode particles. Similar result has been obtained by Srivastava et al. (2012) who found that polluted dust was the dominant aerosol type at Kanpur in central IGB, whereas polluted continental was dominant at Gandhi College in eastern IGB. Dey et al. (2004) have also reported considerable fraction of fine mode aerosols in the volume size distribution over Kanpur during pre-monsoon season. Though the fine mode concentration stayed in $0.05\text{--}0.15\ \mu\text{m}^3\ \mu\text{m}^{-2}$ range during all seasons, they noted a significant increase in the coarse mode during pre-monsoon and monsoon seasons.

3. Instrumentation and analysis

The measurements and sampling were carried out every third day for 8 h during 0900 h–1700 h. Sampling for long durations (e.g. in our case for entire summer) is very demanding on the instruments, especially when sampling is made daily. Sampling on every third day allowed sufficiently large number of samples without any bias for weekdays and weekends. In addition, a log was maintained detailing the prevailing weather and environmental conditions to aid interpretation of the results obtained.

3.1. PM sampling

Sampling of fine ($\text{PM}_{2.5}$) and coarse (PM_{10}) particulate matter were carried out for 8 h with a frequency of close to three times a week. The measurement site was the atmospheric monitoring station (AMS-IIT Kanpur, 26.52°N , 80.23°E) on the top of an existing 25 m high overhead water tank within the Indian Institute of Technology Kanpur premises. Sampling was carried out using PM_{10} , $\text{PM}_{2.5}$ (APM 541, APM 550 Envirotech make) samplers at a constant flow rate of 16.7 LPM. APM 550 model contains a portable Wins-Anderson impactor for the sampling of $\text{PM}_{2.5}$ (Singh et al., 2011; Srimuruganandam and Shiva Nagendra, 2011). The particulate matter was collected on quartz fibre filters (diameter 47 mm) with 37 mm collection diameter and high-retention efficiency. Total 37 samples were collected each for PM_{10} and $\text{PM}_{2.5}$. Filter blanks were also collected after every 10 samples to enhance data quality.

Quartz fibre filters used in the sampling were visually inspected and stored at room temperature for pre-conditioning and post-

conditioning for a period of 24 h to prevent moisture accumulation on the filter surface. Filters were weighed thrice before and after sampling using a six digit micro-balance (Mettler MT5). Filters were handled using fine tweezers and put in filter cases carefully to avoid any contamination. The difference in the pre and post weight is the corresponding PM mass collected on the filter. Dividing mass over volume of air sampled gives PM concentration of particles.

3.2. SMPS and APS

Sub-micron aerosol size distribution from poly-dispersed phases was measured continuously using Scanning Mobility Particle Sizer (SMPS) (TSI, 3080), which covers the particle mobility size range from 14.6 nm to 685 nm. Ambient aerosols are charged using a Kr-85 neutralizer which then enters into the long Differential Mobility Analyzer (long DMA) (TSI 3081) where aerosols are classified on the basis of their electrical mobility. Finally, number concentration of the particles coming out of the DMA is measured by the CPC (TSI, 3775). The sample to aerosol ratio (SAR) is maintained at 10:1. Multiple charge correction and diffusional losses have also been taken into account to overcome over-prediction and under-prediction, respectively.

Size distribution of the particles having continuum regime aerodynamic diameter ranging from $0.5\ \mu\text{m}$ to $20\ \mu\text{m}$ was measured using an Aerodynamic Particle Sizer (APS, 3321) employing time of flight technique, maintained at a flow rate of 5 LPM.

3.3. Chemical analysis

A punch of 16.5 mm filter, cut into small pieces, was digested in a round-bottom flask using 20 mL of HNO_3 (suprapure, Merck), on a hot plate for 2 h at 180°C until small amount of the acid was left (Chakraborty and Gupta, 2010). It was followed by cooling to room temperature and diluted to 100 mL by using Milli Q water (resistivity of $18\ \text{M}\Omega$) and vacuum filtered using a $0.22\ \mu\text{m}$ pore size filter paper and kept in a volumetric flask for subsequent elemental analyses. In total, 13 elements (Ca, Cr, Cu, Fe, K, Mg, Mn, Na, Ni, Pb, Se, V, and Zn) were detected using ICP-OES (Inductively Coupled Plasma Optical Emission Spectroscopy, Thermo fisher, ICAP-6300 duo) (Chakraborty and Gupta, 2010; Gupta and Mandariya, 2013). All the blanks were subjected to the same analysis and used for blank correction.

3.4. PASS and aethalometer

Absorption (β_{abs}) and scattering (β_{scat}) coefficients were obtained directly at 781 nm from Photoacoustic Soot Spectrometer (PASS). The instrument draws the sample air at a flow rate of 1 LPM drawing the particles into the contact of laser beam of 2 W, 781 nm. It works on the principle of photoacoustic effect in which molecules get thermally excited due to light absorption. The absorbed energy is radiated in the form of heat, which produces sound waves due to pressure variation. The sound waves are measured through microphone, and β_{abs} is calculated using simple linear theory. In addition to this, β_{scat} is also measured through a scattering sensor using a photo multiplier tube (PMT) detector, which works on the principle of photoelectric effect. Extinction coefficient (β_{ext}) is obtained by adding β_{abs} and β_{scat} measured at 781 nm. Because single scattering albedo (SSA) is not a direct product from PASS, it is calculated as the ratio of β_{scat} to β_{ext} (Jai Devi et al., 2011; Ram et al., 2012; Shamjad et al., 2012).

The black carbon mass concentration ($\mu\text{g}/\text{m}^3$) was obtained at every 5 min interval from Aethalometer at seven wavelengths in the range 370–950 nm at a flow rate of 2 LPM. The percentage attenuation is directly proportional to the mass of BC deposited on the filter, and is obtained by Beer Lambert law (Shamjad et al., 2012). Filter artifacts such as multiple scattering and shadowing effect of the particles influence the Aethalometer response to light absorbing or scattering particles (Arnott et al., 2005; Weingartner et al., 2003).

4. Results and discussion

We classified the aerosol types encountered during the study period into four categories: background aerosol, mixed aerosol, dust dominated aerosol, and pollution dominated aerosol. We first describe the basis of this classification (Section 4.1), followed by comparison of various aerosol properties for these aerosol types. A detailed discussion on chemical study carried out during this experiment is presented elsewhere by Ghosh et al. (2014).

4.1. Classification of aerosol types

Aerosol types at Kanpur have been classified earlier based on AERONET sunphotometer measurements (Srivastava et al., 2012; Giles et al., 2011). Srivastava et al. (2012) have classified the pre-monsoon aerosol types into five categories: ‘polluted dust’, ‘polluted continental’, ‘mostly black carbon’, ‘mostly organic carbon’, and ‘non-absorbing fine-mode aerosols’. Their classification was based on the density plot of AERONET derived fine mode fraction (FMF) versus single scattering albedo (SSA), and was corroborated by aerosol optical depth (AOD) versus Angstrom exponent (AE) density plot. Giles et al. (2011) have studied the aerosol types classified under categories ‘mostly dust’, ‘mostly BC’, and ‘mixed BC and dust’ based on absorption Angstrom exponent versus extinction Angstrom exponent, and also based on absorption Angstrom exponent versus fine mode fraction.

In the present study, we have attempted to group the aerosol types encountered during the experiment based on in-situ measurements of aerosol physical and chemical properties. It should be noted that during the pre-monsoon season, aerosol loading at Kanpur has considerable fraction of dust as compared to other seasons (Dey et al., 2004; Kaskaoutis et al., 2013). In addition, Kanpur being an industrial location, there is always a contribution from anthropogenic components (Dey et al., 2004). Hence, there is a minimum level of dust and anthropogenic component that is present as background aerosol during the pre-monsoon season. Our categorisation of aerosol types is based on an examination of

the extent to which this background aerosol level is perturbed by enhanced dust loading and/or pollution. It should be noted that these categories are based on surface measurements made during the experiment, hence depending on the absence or presence of elevated aerosol layers, may or may not be consistent with the categories based on AERONET measurements mentioned earlier. The various steps of our classification procedure are as follows (Fig. 4):

STEP 1

In the distribution of PM_{10} concentration, the data points below the 25 percentile correspond to the low aerosol loading days, and are labelled as ‘background aerosol’. For our study, this threshold is $\text{PM}_{10} < 60 \mu\text{g}/\text{m}^3$. Background aerosol encompasses the minimum level of dust along with the pollution component that is always present at the Kanpur location during the pre-monsoon season.

STEP 2

For the other cases, the aerosol loading may have increased due to enhanced dust loading, or pollution, or other processes. So, for the cases remaining after Step 1, Ca concentration was used as a proxy for dust. Highest value of Ca concentration of ‘background aerosol’ category in Step 1 is assumed to be the threshold for dust detection. The value of this Ca threshold for our study is $1.5 \mu\text{g}/\text{m}^3$. The cases which failed this test were termed as ‘uncertain’ or ‘mixed type aerosols’, having no dominant contribution from dust.

STEP 3

The cases which passed the Ca test in Step 2, had signature of dust. These cases were further examined for the BC mass concentration to find the level of pollution mixing with dust. The data points above the 75 percentile in BC distribution correspond to high pollution level. These are classified as ‘pollution dominated aerosol’.

The remaining cases were considered as ‘dust dominated aerosol’. These cases had relatively low level of anthropogenic component, and dust was the dominant species.

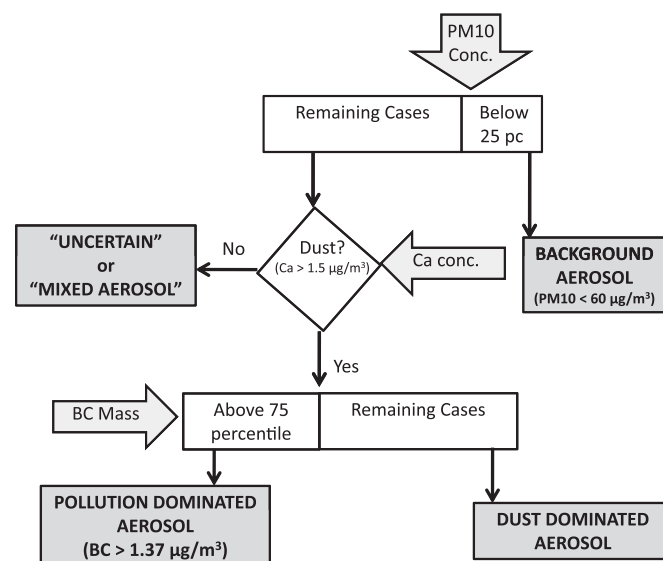


Fig. 4. Flow chart depicting the procedure for classification of aerosol types that was followed in this study.

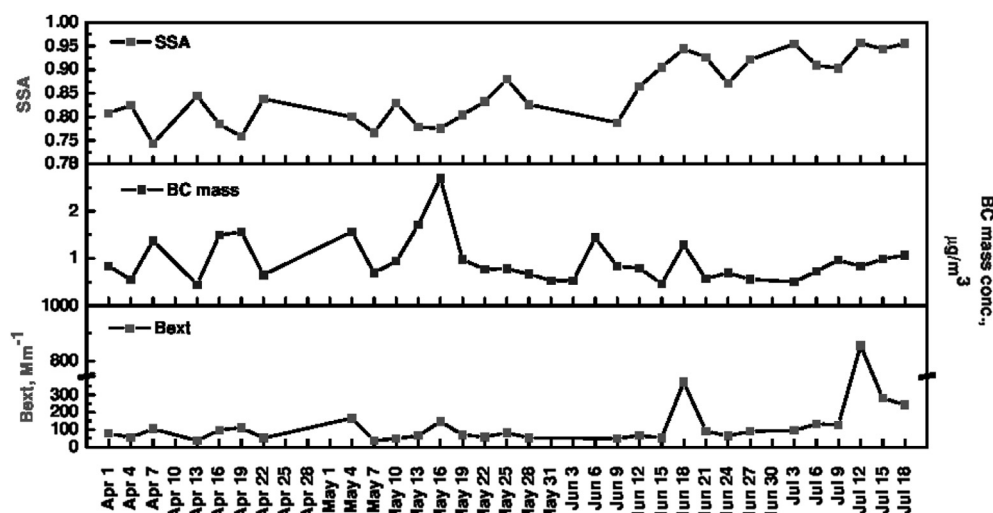


Fig. 5. Time Series of single scattering albedo (SSA) at 781 nm, black carbon (BC) mass, and extinction coefficient (β_{ext}).

This classification is a major highlight of the present work. It attempts to consolidate the various studies on different aspects of dust properties during pre-monsoon season. It attempts to identify dust and distinguish cases of enhanced mixing of dust with anthropogenic component. PM_{10} concentration has been previously used by Ganor et al. (2009) to study dusty days. Ca is known to be an abundant constituent of mineral dust (Ram et al., 2010, 2012). BC is a product of burning and anthropogenic emissions (Bond and Bergstrom, 2006). Out of the 37 sampling days, 8 background aerosol, 12 mixed aerosol, 12 dust dominated, 5 pollution dominated days have been distinctly identified using our aerosol classification from our data.

6 out of 8 background aerosol cases belonged to end of June, and July. During late pre-monsoon season, several processes are at play, which have effect on the aerosol loading in the atmosphere. Rainfall is likely to play a role in controlling the aerosol concentration in the atmosphere. Heavy rainfall can wash out aerosols from the atmosphere. Alternatively, heavy rainfall will result in moist soils which in turn will decrease the amount of soil-generated aerosols. However, high humidity leads to hygroscopic growth of aerosols. Conversion of sulphur dioxide to sulphate aerosols is also faster in high humidity conditions. The resulting aerosol climatology depends on the dominant process.

Dust dominated days had representation from April, May, and June months, whereas pollution dominated cases belonged only to April and May. The study period of pre-monsoon coincides with the peak season of cement industry. Both the demand and supply of cement is high in this region during this season owing to large-scale construction activities. Cement is a contributor of dust aerosols at its production, transport, and usage stage (during construction work). Besides roadside dust, the dust from barren agricultural field is also a potential source. We did not encounter any dust related day after 21 June in our study – neither in dust dominated aerosol category, nor in pollution dominated aerosol category. This could be due to the removal processes taking place after onset of monsoon as described previously. The anthropogenic component from industrial and vehicular emission is a source of pollution mixing with dust, in the pollution dominated aerosol category. In addition, the forest fires prevalent in Nepal during April and May lead to enhanced pollution mixing on the days when air mass from those regions gets transported to the sampling location. A comparative examination of different aerosol properties for these categories are presented later. Note that the ‘dust dominated

aerosol’ category described above corresponds to the ‘dust’ category defined by Ghosh et al. (2014); ‘background aerosol’ to the ‘continental aerosol’ category, and ‘pollution dominated aerosol’ combines the polluted dust 1 and polluted dust 2 categories of Ghosh et al. (2014).

4.2. SSA, β_{ext} , and BC mass

SSA (at 781 nm) and β_{ext} of ambient aerosol were obtained from the PASS by the methods described earlier. Time series of SSA, β_{ext} , and BC mass concentration are shown in Fig. 5. SSA value of 1 corresponds to purely scattering species, while 0 refers to purely absorbing particles. The average values of SSA and β_{ext} during April, May, June, and July were found to be 0.79 ± 0.03 , 0.81 ± 0.03 , 0.88 ± 0.05 , 0.93 ± 0.02 and $76.8 \pm 27.2 \text{ Mm}^{-1}$, $80.4 \pm 45.3 \text{ Mm}^{-1}$, $112.3 \pm 116.1 \text{ Mm}^{-1}$, $288.9 \pm 287.0 \text{ Mm}^{-1}$, respectively. In June and July, β_{abs} reduced nearly half the value in April and May, while β_{ext} almost got doubled. The maximum value of SSA was obtained in July, which reflects larger contribution of scattering particles to the overall extinction. From pre-monsoon (April, May) to monsoon (June, July) period, SSA increased from 0.76 to 0.95, while β_{ext} showed a three fold increase.

The increase in SSA and β_{ext} during late June and July is similar to the increase observed in RH. One possibility of higher SSA during July could be hygroscopic growth of particles. However, no corresponding increase in PM_{10} concentration is noticed in our data. Another possibility is the change in dominant aerosol type during July. As discussed later in Section 4.5, air mass in July have origin in Arabian Sea, Bay of Bengal, or delta region of Ganga. Thus, sea salt aerosol is a significant contributor to aerosol samples collected during July, as compared to dust during April to June. Sea salt aerosols are less absorbing than dust and are hygroscopic in nature. The concentration of dust aerosols is low during July due to wash out and wet soil. Thus the overall aerosols in July are of more scattering nature than the other three months studied.

The averages of BC mass concentrations were $1.25 \pm 0.81 \mu\text{g}/\text{m}^3$, $1.17 \pm 0.65 \mu\text{g}/\text{m}^3$, $0.79 \pm 0.34 \mu\text{g}/\text{m}^3$, and $0.84 \pm 0.20 \mu\text{g}/\text{m}^3$ in April, May, June, and July, respectively. The lower value of BC mass concentration for June and July denotes lower pollution levels, which is reflected by corresponding increase in the SSA values for June and July compared to that in April and May. The source of BC could be local vehicular emission, or forest fire in Nepal region that was prevalent during the studied season. Large variation in BC mass was

Table 1

Average and standard deviation of SSA, BC mass concentration, PM₁₀ concentration, and coarse mode fraction for the four aerosol categories defined in this study.

Aerosol type	SSA	BC	PM ₁₀	Coarse mode fraction
Background aerosols	0.87 ± 0.07	0.83 ± 0.19	44.93 ± 12.35	0.37 ± 0.12
Dust dominated aerosols	0.85 ± 0.06	0.79 ± 0.23	107.45 ± 44.56	0.59 ± 0.22
Mixed aerosols	0.84 ± 0.09	1.23 ± 0.95	110.35 ± 49.42	0.59 ± 0.15
Pollution dominated aerosols	0.76 ± 0.02	1.59 ± 0.08	151.81 ± 73.60	0.74 ± 0.10

noted during the experiment. However, after 21 June, there was a steady and very small increase in BC mass, with its value remaining below 1.02 µg/m³. [Shamjad et al. \(2012\)](#) have shown that there could be coating by water droplet on BC particles, especially under high humidity conditions, leading to enhanced absorption.

As noted previously, the cases with high levels of BC have been classified as pollution dominated aerosol, which imply pollution mixing with dust. However, for three days (7 April, 25 April, and 16 May), we observed very high BC mass and low dust loading. This could be either due to the enhanced absorption by water coating on BC particles, or aerosols originating from burning events taking place in Nepal forests. However, as they do not involve any dust signature which is the focus of our study, we have classified these dates in mixed aerosol category.

Average BC mass was highest for pollution dominated aerosols (1.59 ± 0.08 µg/m³), which is expected because this aerosol category was defined on the basis of above 75 percentile data points in the BC mass concentration. A noticeable feature is the presence of significant amount of BC in all aerosol categories ([Table 1](#)). As mentioned previously, Kanpur is an industrial city so that vehicular and industrial emission is present throughout the year, with varying amounts. Largest variation (highest standard deviation) in BC mass was noted for mixed aerosol category (SD = 0.95). This is on account of the three days of high pollution level and low dust loading mentioned in the previous paragraph. BC mass on dust dominated days (0.79 ± 0.23 µg/m³) was lower than the

background aerosol (0.83 ± 0.19 µg/m³) category, hence it can be taken as the background contribution.

Highest SSA were observed for the background aerosols (0.87 ± 0.07). As noted previously, sea salt aerosols, which are largely scattering in nature, had significant contribution to the background aerosol class. Lowest SSA were noted for pollution dominated aerosols (0.76 ± 0.02), mainly because of absorbing nature of anthropogenic aerosols governing this category. Though average SSA of mixed aerosols (0.84 ± 0.09) and dust dominated aerosols (0.85 ± 0.06) were nearly similar, there was a large variation (standard deviation) in the case of mixed aerosols. This is on account of the variety of aerosols in this category – there are cases of high anthropogenic component which are essentially absorbing in nature, and also cases of sea-salt aerosols in late June and July, which are largely scattering in nature. With advancement of season, there is large change in relative humidity, so that scattering properties of hygroscopic aerosols also changes. The average values of SSA and BC mass for different aerosol categories are given in [Table 1](#), along with PM₁₀ concentration and coarse mode fraction which are discussed in the next section.

4.3. Size distribution

The seasonal average PM₁₀ was 2.7 times higher to PM_{2.5} during the campaign period. Average PM₁₀ during April, May, June, and July months was noted to be 98.47 ± 53.62, 137.17 ± 65.06, 89.38 ± 29.33, and 50.95 ± 18.44 µg/m³, respectively. The quantity PM₁₀–PM_{2.5}/PM₁₀, defined as the coarse mode fraction (CMF), was observed to be 0.62 ± 0.19, 0.68 ± 0.13, 0.48 ± 0.16, and 0.33 ± 0.11 during April, May, June, and July months, respectively. Based on observations at Delhi during August 2007 to October 2008, [Tiwari et al. \(2012\)](#) have reported summertime PM₁₀ values to be 8% higher than PM_{2.5}.

The average PM₁₀ concentration was highest for the pollution dominated aerosol category (151.81 ± 73.60 µg/m³). The CMF was also highest for pollution dominated aerosol category (0.74 ± 0.10). Thus, in spite of high anthropogenic contribution to this category, dust remained the dominant species. As described previously,

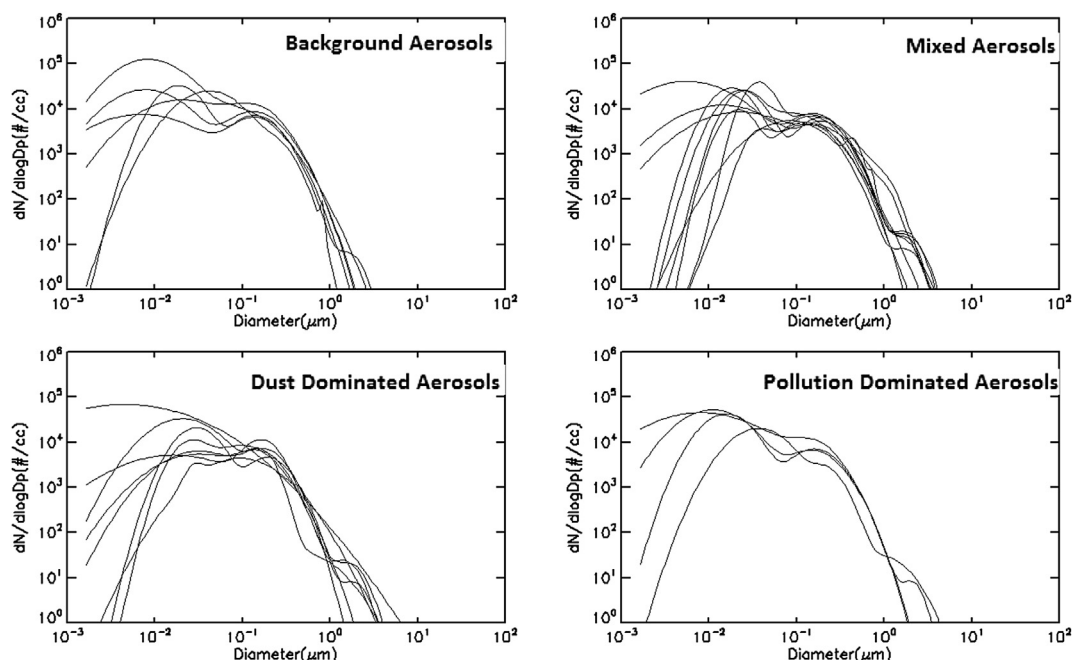


Fig. 6. Aerosol size distributions for the background aerosols, mixed aerosols, dust dominated aerosols, and pollution dominated aerosols categories.

pollution dominated aerosols are same as the dust dominated aerosols, except that the former have very high BC concentration, thereby implying higher mixing of dust with pollution aerosols. Thus, both of these aerosol categories would contain considerable fraction of coarse mode particles.

The standard deviation of CMF for pollution dominated aerosols was lower than other classes suggesting that there was less variation of large size particles in this category. The standard deviation of PM_{10} concentration was large for pollution dominated aerosols. Thus, there was a large variation in total aerosol loading on the days belonging to this category. Since the variation in coarse mode fraction was less, it implies considerable variation in the concentration of anthropogenic component for this class.

PM_{10} concentration and CMF of mixed aerosols ($PM_{10} = 110.35 \pm 49.42 \mu\text{g}/\text{m}^3$, $\text{CMF} = 0.59 \pm 0.15$) were slightly higher than dust dominated aerosols ($PM_{10} = 107.45 \pm 44.56 \mu\text{g}/\text{m}^3$, $\text{CMF} = 0.59 \pm 0.22$). Among all categories, coarse mode fraction had highest variation (largest standard deviation) for dust dominated aerosols. This implies contribution from different sizes and types of dust to this category. PM_{10} concentration being lowest for background aerosols ($44.93 \pm 12.35 \mu\text{g}/\text{m}^3$) was expected as this category was defined on the basis of below 25 percentile data points in the PM_{10} concentration.

The size distribution from SMPS and APS was merged into a single size distribution (14.6 nm–20 μm) using the TSI Aerosol Instrument Manager Program Data merge software module version 3.0.1.0. The merging process removes the discontinuity in the number distribution (Jai Devi et al., 2011). We have taken into account the inherent difference between the mobility size measured by the SMPS and aerodynamic diameter measured by the APS. During the merging, shape factor of 1 and density of bulk atmospheric aerosols equal to 1.6 g/cc has been used.

Mostly bimodal and trimodal distributions were observed (Fig. 6). The maximum particle diameter was noted to have increased for dust dominated aerosols, mixed aerosols, and pollution dominated aerosols as compared to the background aerosols. The peak of the fine mode was at 0.01 μm for background aerosols and pollution dominated aerosols. This peak increased towards larger particle size in the case of mixed aerosols and dust dominated aerosols. Thus, background aerosols and pollution dominated aerosols had a larger fraction of finer particles as compared to dust dominated and mixed aerosol types. A noticeable feature is the presence of coarse mode and fine mode particles in all aerosol categories (Fig. 6).

4.4. Chemical composition

The results of elemental analysis of aerosols in $PM_{2.5}$ and PM_{10} samples are depicted in Fig. 7. In total, 13 elements (Ca, Cr, Cu, Fe, K, Mg, Mn, Na, Ni, Pb, Se, V, and Zn) were detected using ICP-OES. The error bars in the figure show variability in the elemental concentrations during this study period. Ca, Fe, Mg, Na contents were high for dust dominated aerosols, a feature more prominent in PM_{10} . Ca, Mg, and Fe are representative of mineral dust, and mainly have crustal origin. Na can come from salt-affected land (sodic soil) which are evenly distributed in Indo-Gangetic basin (Kumar and Sarin, 2010). On the other hand, pollution dominated aerosols were enriched with the anthropogenic elements like Cr, Cu, Mn, Ni, Pb, Se, V, and Zn. Anthropogenic elements are fine particles having longer suspension or residence time compared to coarse particles, and are more prominent in fine mode $PM_{2.5}$. Elemental concentration in mixed aerosols was found higher than background aerosols, but intermediate to dust dominated and pollution dominated aerosols. Lowest elemental concentrations were observed for background aerosols.

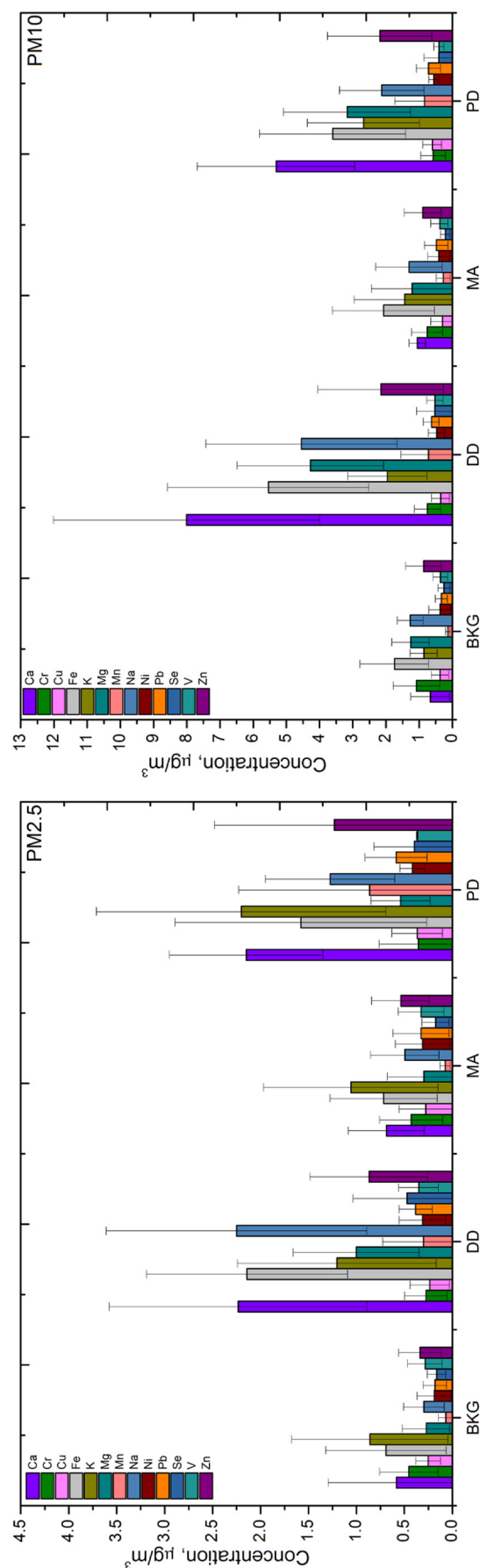


Fig. 7. Results of elemental analysis of $PM_{2.5}$ and PM_{10} samples, respectively, collected during the campaign. BKG, DD, MA, and PD denote background aerosols, dust dominated aerosols, mixed aerosols, and pollution dominated aerosols categories, respectively. See text for more discussion.

In our samples, $(\text{Ca}/\text{Fe})_{\text{PM}_{10}}$ ratio varied between 0.21–3.83, (mean value = 1.26), and $(\text{Ca}/\text{Fe})_{\text{PM}_{2.5}}$ ratio varied between 0.11–2.83, (mean value = 1.09). These ratios are close to that found in the upper continental crust (UCC) i.e. 0.89 (Rudnick and Gao, 2003), and reflect signature of dust. The values higher than UCC are possibly due to contribution from calcium carbonate dominated Ganga river sediments.

Here we have provided the broad features observed in the chemical analysis of the samples collected. For detailed presentation of chemical composition, the reader may refer to Ghosh et al. (2014).

4.5. Backtrajectories and sources

In order to identify the sources of the aerosols sampled, 10 day HYSPLIT backtrajectory analysis at 25 m height and 0800 h GMT, starting at the measurement location, was performed (Fig. 8) (Draxler and Hess, 2005). The meteorological data was taken from NCEP Reanalysis (Kalnay et al., 1996). Backtrajectory analysis of all the cases reveals the dominance of local aerosols, though sea-salt and long-range transported aerosols are also present. Backtrajectories during July were mostly of oceanic origin, having originated in either Bay of Bengal or the Arabian Sea.

In none of the cases of background aerosol type, the air mass had crossed any desert or dust dominated area. Among the cases belonging to background aerosol type, in 5 cases, the air mass either originated from the oceans, or from the Gangetic delta. Besides, the air mass had local origin in one case, and in another the air mass originated in Nepal. Thus, the background aerosols encompassed aerosols of diverse types and origin. In the mixed aerosol cases in late June and July, the air mass had oceanic origin. This implies a possibility of sea salt aerosols being transported to the sampling location. Sea salt aerosols are hygroscopic in nature, which in high humidity condition, typical during late June and July, can grow in size with further implication on scattering properties. The hygroscopic growth of these aerosols could be one mechanism

whereby mixed aerosols had high PM_{10} concentration, though no signature of dust was present in them. No oceanic origin of air mass sampled on dust dominated and pollution dominated days was noticed. Hence, in general, the aerosol types identified by our classification scheme are consistent with the sources identified by backtrajectory analysis.

Most backtrajectories showed the aerosols sampled to be of local origin. These had mostly originated from the Indo Gangetic basin itself, and in a few cases from the Thar desert. Besides, in two mixed aerosol cases, and in 5 dust dominated cases, the trajectories showed 'short range' transport – having originated in neighbouring Pakistan or Afghanistan. However, we have encountered cases of long range transport of aerosols also. In three cases, one each in the dust dominated aerosol (25 May), mixed aerosol (16 May), and pollution dominated aerosol (13 May) categories, the air mass had crossed west Asia, a region dominated by dust aerosols. The backtrajectory ending on 25 May (dust dominated aerosol case) had also crossed north east Africa before following the path via west Asia to enter India. Dust in this region is rich in Ca, consistent with our classification. The trajectory ending on 13 May (pollution dominated aerosol case) also was associated with high Ca dust in north Africa, a feature reflected in our data also. However, there was enhanced mixing of this air mass with pollution so that this date was classified as pollution dominated aerosol. Though the backtrajectory ending on 16 May (mixed aerosol case) had origin in dust dominated north Africa and west Asia, this is not reflected in our data. The Ca content was observed to be at the background aerosol level, and no enhanced dust contribution was observed.

In summary, though majority of cases implied aerosols of local origin, there were also cases of short-range (originating in Pakistan or Afghanistan) and long-range transport (originating from or crossing over west Asia). Trajectories of oceanic origin in Bay of Bengal, Arabian Sea, or delta region of Ganga were also encountered. Trajectories originating in the forest fire affected region of Nepal, and highly polluted Delhi and neighbouring areas were associated with pollution dominated aerosols. Thus, the aerosol

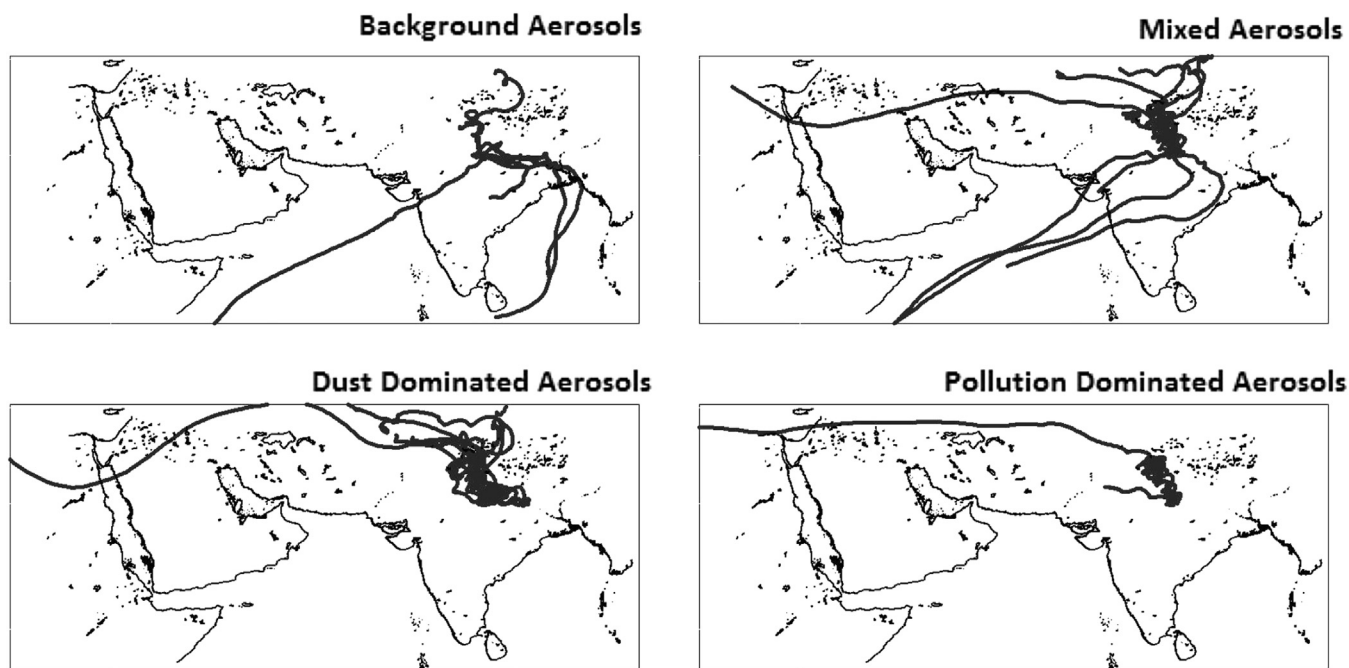


Fig. 8. 10-day air mass backtrajectories ending on days belonging to the background aerosols, mixed aerosols, dust dominated aerosols, and pollution dominated aerosols categories.

climatology of the study region during pre-monsoon season encompasses different aerosols with widely varying properties and having different sources. This diversity in aerosol sources is reflected in our data, and is consistent with our scheme for classification of aerosol types.

5. Conclusions

Based on the measurement during a four month period from April to July 2011, various aspects of dust properties at Kanpur in the Indo-Gangetic basin were studied. Based on PM₁₀ concentration, BC mass and Ca concentrations, the aerosol types encountered during the experiment were classified into four categories: background aerosol, dust dominated aerosol, pollution dominated aerosol, and mixed aerosol. Background aerosols represent the minimum level of dust and pollution loading that is always present at Kanpur during the pre-monsoon season. Dust dominated aerosols, identified by higher Ca concentration, represent enhanced dust loading in the atmosphere. Pollution dominated aerosols, containing higher BC mass, represent enhanced mixing of dust with pollution. Mixed aerosols represent higher aerosol loading which was not associated with dust. In addition to the presence of locally generated aerosols, both short-range transported and long-range transported aerosols were also detected. The classification of aerosol types was found consistent with various aerosol properties examined and the backtrajectory analysis. Total concentration of elements was high during dust dominated days, and low during background aerosol days. Concentration of typical crustal elements such as Ca, Fe, Mg were high during dust dominated days. Pollution dominated aerosols were enriched with anthropogenic elements like Zn, V, Se, Cr. These findings lead to a better understanding of aerosol climatology over the Indo-Gangetic basin during pre-monsoon season, and have further applications in the study of dust transport, and dust radiative effect.

Acknowledgements

The authors gratefully acknowledge the NOAA Air Resources Laboratory (ARL) for the provision of the HYSPLIT transport and dispersion model and READY website (<http://www.ready.noaa.gov>) used in this publication. NCEP Reanalysis data was provided by the ESRL PSD, Boulder, Colorado, USA, from their website at <http://www.esrl.noaa.gov/psd/>. The GrADS script used for plotting wind rose diagram was written by Warren Tennant. Map of study region was obtained from Google Earth. This work is partially funded by the National Academy of Sciences. The conclusions derived from this work are those of the authors alone, and do not reflect the views of the NAS.

Appendix A. Supplementary data

Supplementary data related to this article can be found at <http://dx.doi.org/10.1016/j.atmosenv.2014.08.043>.

References

- Arnott, W.P., Hamasha, K., Moosmüller, H., Sheridan, P.J., Ogren, J.A., 2005. Towards aerosol light-absorption measurements with a 7-wavelength aethalometer: evaluation with a photoacoustic instrument and 3-wavelength nephelometer. *Aerosol Sci. Technol.* 39 (1), 17–29.
- Bond, T.C., Bergstrom, R.W., 2006. Light absorption by carbonaceous particles: an investigative review. *Aerosol Sci. Technol.* 40 (1), 27–67.
- Chakraborty, A., Gupta, T., 2010. Chemical characterization and source apportionment of submicron (PM₁) aerosol in Kanpur region, India. *Aerosol Air Qual. Res.* 10 (5), 433–445.
- Chen, G., Ziemba, L.D., Chu, D.A., Thornhill, K.L., Schuster, G.L., Winstead, E.L., Diskin, G.S., Ferrare, R.A., Burton, S.P., Ismail, S., Kooi, S.A., Omar, A.H., Slusher, D.L., Kleb, M.M., Reid, J.S., Twohy, C.H., Zhang, H., Anderson, B.E., Jan. 2011. Observations of Saharan dust microphysical and optical properties from the Eastern Atlantic during NAMMA airborne field campaign. *Atmos. Chem. Phys.* 11, 723–740. <http://dx.doi.org/10.5194/acp-11-723-2011>.
- Chinnam, N., Dey, S., Tripathi, S.N., Sharma, M., Apr. 2006. Dust events in Kanpur, northern India: chemical evidence for source and implications to radiative forcing. *Geophys. Res. Lett.* 33, L08803. <http://dx.doi.org/10.1029/2005GL025278>.
- Choudhry, P., Misra, A., Tripathi, S.N., 2012. Study of MODIS derived AOD at three different locations in the Indo Gangetic Plain: Kanpur, Gandhi College and Nainital. *Ann. Geophys.* 30, 1479–1493. <http://dx.doi.org/10.5194/angeo-30-1479-2012>.
- Chowdhury, P.K.R., Maithani, S., Dadhwal, V.K., 2012. Estimation of urban population in Indo-Gangetic Plains using night-time OLS data. *Int. J. Remote Sens.* 33 (8), 2498–2515.
- Dey, S., Tripathi, S.N., Singh, R.P., Holben, B.N., Oct. 2004. Influence of dust storms on the aerosol optical properties over the Indo-Gangetic basin. *J. Geophys. Res. (Atmos.)* 109, 20211. <http://dx.doi.org/10.1029/2004JD004924>.
- Draxler, R.R., Hess, G.D., 2005. An overview of the HYSPLIT 4 modelling system for trajectories, dispersion, and deposition. *Aust. Meteor. Mag.* 47, 295–308.
- Eck, T.F., Holben, B.N., Sinyuk, A., Pinker, R.T., Goloub, P., Chen, H., Chatenet, B., Li, Z., Singh, R.P., Tripathi, S.N., Reid, J.S., Giles, D.M., Dubovik, O., O'Neill, N.T., Smirnov, A., Wang, P., Xia, X., Oct. 2010. Climatological aspects of the optical properties of fine/coarse mode aerosol mixtures. *J. Geophys. Res. (Atmos.)* 115, 19205. <http://dx.doi.org/10.1029/2010JD014002>.
- Formenti, P., Schütz, L., Balkanski, Y., Desbois, K., Ebert, M., Kandler, K., Petzold, A., Scheuven, D., Weinbruch, S., Zhang, D., Aug. 2011. Recent progress in understanding physical and chemical properties of African and Asian mineral dust. *Atmos. Chem. Phys.* 11, 8231–8256. <http://dx.doi.org/10.5194/acp-11-8231-2011>.
- Ganor, E., Stupp, A., Alpert, P., 2009. A method to determine the effect of mineral dust aerosols on air quality. *Atmos. Environ.* 43, 5463–5468. <http://dx.doi.org/10.1016/j.atmosenv.2009.07.028>.
- Ghosh, S., Gupta, T., Rastogi, N., Gaur, A., Misra, A., Tripathi, S.N., Paul, D., Tare, V., Prakash, O., Bhattu, D., Dwivedi, A.K., Kaul, D.S., Dalai, R., Mishra, S.K., 2014. Chemical characterization of summertime dust events at Kanpur: insight into the sources and level of mixing with anthropogenic emissions. *Aerosol Air Qual. Res.* 14, 879–891.
- Giles, D.M., Holben, B.N., Tripathi, S.N., Eck, T.F., Newcomb, W.W., Slutsker, I., Dickerson, R.R., Thompson, A.M., Mattoo, S., Wang, S.-H., Singh, R.P., Sinyuk, A., Schafer, J.S., Sep. 2011. Aerosol properties over the Indo-Gangetic Plain: a mesoscale perspective from the TIGERZ experiment. *J. Geophys. Res. (Atmos.)* 116, 18203. <http://dx.doi.org/10.1029/2011JD015809>.
- Gupta, T., Mandariya, A., 2013. Sources of submicron aerosol during fog-dominated wintertime at Kanpur. *Environ. Sci. Pollut. Res.*, 1–15. <http://dx.doi.org/10.1007/s11356-013-1580-6>.
- Jai Devi, J., Tripathi, S.N., Gupta, T., Singh, B.N., Gopalakrishnan, V., Dey, S., 2011. Observation-based 3-D view of aerosol radiative properties over Indian Continental Tropical Convergence Zone: implications to regional climate. *Tellus B* 63 (5), 971–989.
- Kalnay, E., Kanamitsu, M., Kistler, R., Collins, W., Deaven, D., Gandin, L., Iredell, M., Saha, S., White, G., Woollen, J., et al., 1996. The ncep/ncar 40-year reanalysis project. *Bull. Am. Meteorol. Soc.* 77 (3), 437–471.
- Karanasiou, A., Moreno, N., Moreno, T., Viana, M., de Leeuw, F., Querol, X., 2012. Health effects from sahara dust episodes in Europe: literature review and research gaps. *Environ. Int.* 47, 107–114.
- Karydis, V.A., Kumar, P., Barahona, D., Sokolik, I.N., Nenes, A., Dec. 2011. On the effect of dust particles on global cloud condensation nuclei and cloud droplet number. *J. Geophys. Res. (Atmos.)* 116, 23204. <http://dx.doi.org/10.1029/2011JD016283>.
- Kaskaoutis, D.G., Sinha, P.R., Vinoj, V., Kosmopoulos, P.G., Tripathi, S.N., Misra, A., Sharma, M., Singh, R.P., Nov. 2013. Aerosol properties and radiative forcing over Kanpur during severe aerosol loading conditions. *Atmos. Environ.* 79, 7–19. <http://dx.doi.org/10.1016/j.atmosenv.2013.06.020>.
- Kaufman, Y.J., Koren, I., Remer, L.A., Tanré, D., Ginoux, P., Fan, S., Feb. 2005. Dust transport and deposition observed from the Terra-Moderate Resolution Imaging Spectroradiometer (MODIS) spacecraft over the Atlantic Ocean. *J. Geophys. Res. (Atmos.)* 110, 10. <http://dx.doi.org/10.1029/2003JD004436>.
- Kumar, A., Sarin, M., 2010. Atmospheric water-soluble constituents in fine and coarse mode aerosols from high-altitude site in western India: long-range transport and seasonal variability. *Atmos. Environ.* 44 (10), 1245–1254.
- Mishra, S.K., Tripathi, S.N., Dec. 2008. Modeling optical properties of mineral dust over the Indian Desert. *J. Geophys. Res. (Atmos.)* 113, 23201. <http://dx.doi.org/10.1029/2008JD010048>.
- Misra, A., Tripathi, S.N., Kaul, D.S., Welton, E.J., 2012. Study of MPLNET-derived aerosol climatology over Kanpur, India, and Validation of CALIPSO level 2 version 3 Backscatter and extinction products. *J. Atmos. Ocean. Technol.* 29, 12851294. <http://dx.doi.org/10.1175/JTECH-D-11-00162.1>.
- Onishi, K., Kurosaki, Y., Otani, S., Yoshida, A., Sugimoto, N., Kurozawa, Y., Mar. 2012. Atmospheric transport route determines components of Asian dust and health effects in Japan. *Atmos. Environ.* 49, 94–102. <http://dx.doi.org/10.1016/j.atmosenv.2011.12.018>.
- Ram, K., Sarin, M.M., Hegde, P., Dec. 2010. Long-term record of aerosol optical properties and chemical composition from a high-altitude site (Manora Peak) in Central Himalaya. *Atmos. Chem. Phys.* 10, 11791–11803. <http://dx.doi.org/10.5194/acp-10-11791-2010>.
- Ram, K., Sarin, M.M., Tripathi, S.N., 2012. Temporal trends in atmospheric PM_{2.5}, PM₁₀, elemental carbon, organic carbon, water-soluble organic carbon, and

- optical Properties: impact of biomass burning emissions in the indo-gangetic Plain. *Environ. Sci. Technol.* 46 (2), 686–695.
- Reid, J.S., Jonsson, H.H., Maring, H.B., Smirnov, A., Savoie, D.L., Cliff, S.S., Reid, E.A., Livingston, J.M., Meier, M.M., Dubovik, O., Tsay, S.-C., Jul. 2003. Comparison of size and morphological measurements of coarse mode dust particles from Africa. *J. Geophys. Res. (Atmos.)* 108, 8593. <http://dx.doi.org/10.1029/2002JD002485>.
- Reid, J.S., Reid, E.A., Walker, A., Piketh, S., Cliff, S., Al Mandoos, A., Tsay, S.-C., Eck, T.F., Jul. 2008. Dynamics of southwest Asian dust particle size characteristics with implications for global dust research. *J. Geophys. Res. (Atmos.)* 113, 14212. <http://dx.doi.org/10.1029/2007JD009752>.
- Rudnick, R.L., Gao, S., Dec. 2003. Composition of the Continental crust. *Treatise Geochem.* 3, 1–64. <http://dx.doi.org/10.1016/B0-08-043751-6/03016-4>.
- Shamjad, P.M., Tripathi, S.N., Aggarwal, S.G., Mishra, S.K., Joshi, M., Khan, A., Sapra, B.K., Ram, K., 2012. Comparison of experimental and modeled absorption enhancement by black carbon (BC) cored polydisperse aerosols under hygroscopic conditions. *Environ. Sci. Technol.* 46 (15), 8082–8089. <http://dx.doi.org/10.1021/es300295v>.
- Singh, D.P., Gadi, R., Mandal, T.K., Dec. 2011. Characterization of particulate-bound polycyclic aromatic hydrocarbons and trace metals composition of urban air in Delhi, India. *Atmos. Environ.* 45, 7653–7663. <http://dx.doi.org/10.1016/j.atmosenv.2011.02.058>.
- Srimuruganandam, B., Shiva Nagendra, S.M., 2011. Chemical characterization of PM₁₀ and PM_{2.5} mass concentrations emitted by heterogeneous traffic. *Sci. Total Environ.* 409 (17), 3144–3157.
- Srivastava, A.K., Tripathi, S.N., Dey, S., Kanawade, V.P., Tiwari, S., Jun. 2012. Inferring aerosol types over the Indo-Gangetic Basin from ground based sunphotometer measurements. *Atmos. Res.* 109, 64–75. <http://dx.doi.org/10.1016/j.atmosres.2012.02.010>.
- Thorsteinsson, T., Gísladóttir, G., Bullard, J., McTainsh, G., Oct. 2011. Dust storm contributions to airborne particulate matter in Reykjavík, Iceland. *Atmos. Environ.* 45, 5924–5933. <http://dx.doi.org/10.1016/j.atmosenv.2011.05.023>.
- Tiwari, S., Chate, D., Srivastava, A., Bisht, D., Padmanabhamurty, B., 2012. Assessments of PM₁, PM_{2.5} and PM₁₀ concentrations in delhi at different mean cycles. *Geofizika* 29, 125–141.
- Tiwari, S., Srivastava, A., Singh, A., 2013. Heterogeneity in pre-monsoon aerosol characteristics over the indo-gangetic basin. *Atmos. Environ.* 77, 738–747.
- Tripathi, S.N., Dey, S., Tare, V., Satheesh, S.K., 2005. Aerosol black carbon radiative forcing at an industrial city in northern India. *Geophys. Res. Lett.* 32 (8), L08802.
- Weingartner, E., Saathoff, H., Schnaiter, M., Streit, N., Bitnar, B., Baltensperger, U., 2003. Absorption of light by soot particles: determination of the absorption coefficient by means of aethalometers. *J. Aerosol Sci.* 34 (10), 1445–1463.
- Zhang, H., McFarquhar, G.M., Cotton, W.R., Deng, Y., Mar. 2009. Direct and indirect impacts of Saharan dust acting as cloud condensation nuclei on tropical cyclone eyewall development. *Geophys. Res. Lett.* 36, 6802. <http://dx.doi.org/10.1029/2009GL037276>.